

Trace element abundances in the Rock Canyon Anticline, Pueblo, Colorado, marine sedimentary section and their relationship to Caribbean plateau construction and oxygen anoxic event 2

Laura J. Snow¹ and Robert A. Duncan

College of Oceanic and Atmospheric Sciences, Oregon State University, Corvallis, Oregon, USA

Timothy J. Bralower

Department of Geosciences, Pennsylvania State University, University Park, Pennsylvania, USA

Received 16 September 2004; revised 25 January 2005; accepted 4 April 2005; published 4 August 2005.

[1] Rapid eruption of submarine lava flows during formation of the Caribbean plateau correlates closely with ocean anoxic event 2 (OAE2), which bracketed the Cenomanian/Turonian boundary (~93.5 Ma). These events also correspond with a positive excursion in carbon isotopic composition of seawater. Hydrothermal activity associated with large-scale submarine volcanism may have been responsible for this abrupt change in ocean chemistry. We determined the distribution of major, minor, and trace element abundances in the Rock Canyon marine sedimentary section (Pueblo, Colorado). After normalizing element concentrations to Zr to remove the variable contribution of terrigenous material to these sediments, we detected an interval of concentrated metal abundance anomalies that coincides with the abrupt beginning of the positive $\delta^{13}\text{C}$ isotope excursion. The metal abundance anomalies indicate that intermittent hydrothermal activity, in the form of both water/rock exchange and magmatic degassing, introduced large concentrations of trace metals into the Cretaceous ocean at the same time that extinctions of benthic species, turnover in plankton communities, and increases in isotopically light organic carbon burial occurred. The stratigraphic position of this interval of trace metal anomalies matches events associated with OAE2 and indicates that intermittent hydrothermal activity on a massive scale triggered abrupt changes in carbon burial and deep ocean oxygen contents.

Citation: Snow, L. J., R. A. Duncan, and T. J. Bralower (2005), Trace element abundances in the Rock Canyon Anticline, Pueblo, Colorado, marine sedimentary section and their relationship to Caribbean plateau construction and oxygen anoxic event 2, *Paleoceanography*, 20, PA3005, doi:10.1029/2004PA001093.

1. Introduction

[2] One of the most intriguing features of the Cretaceous ocean was the interruption of normal pelagic sediment deposition by several distinct episodes of ocean-wide anoxia [*Schlanger and Jenkyns*, 1976; *Jenkyns*, 1980; *Arthur et al.*, 1990]. These intervals are characterized by finely laminated, organic-rich sediments deposited in oxygen-deficient conditions, accompanied by a positive $\delta^{13}\text{C}$ isotopic excursion in both carbonate and organic carbon sediment fractions [*Scholle and Arthur*, 1980; *Pratt and Threlkeld*, 1984]. *Schlanger and Jenkyns* [1976] termed these periods “oceanic anoxic events” (OAEs). Over the past 3 decades, the origin of these black shales and the geological and climatic processes that brought them about has been vigorously debated.

[3] The marine sedimentary record reveals that the Cretaceous OAEs correlate with a number of changes in ocean chemistry, such as the isotopic composition of strontium (Figure 1) and carbon. Seawater $^{87}\text{Sr}/^{86}\text{Sr}$ values record a

balance between the contributions to strontium in seawater from hydrothermal activity ($^{87}\text{Sr}/^{86}\text{Sr} \sim 0.704$), the weathering of old sialic rocks of the continental crust ($^{87}\text{Sr}/^{86}\text{Sr} \sim 0.720$), and the weathering of marine carbonate rocks ($^{87}\text{Sr}/^{86}\text{Sr} \sim 0.708$). The decreases in seawater $^{87}\text{Sr}/^{86}\text{Sr}$ starting at ~122 Ma and ~94 Ma are most likely the result of an increased flux of hydrothermal Sr into the ocean, because of increased ocean crustal production, rather than a decrease in the chemical weathering of continental rocks [*Ingram et al.*, 1994; *Jones et al.*, 1994; *McArthur et al.*, 1994; *Bralower et al.*, 1997; *Jones and Jenkyns*, 2001]. These negative excursions in the seawater $^{87}\text{Sr}/^{86}\text{Sr}$ are much broader than the OAEs, a feature that results from the long residence time of Sr in the ocean (~5 Ma).

[4] The positive carbon isotopic excursions are widely interpreted as the response of the ocean to enhanced preservation and burial of organic carbon in sediments [e.g., *Scholle and Arthur*, 1980; *Arthur et al.*, 1987]. Biologically synthesized marine organic matter is enriched in ^{12}C , so its removal will cause the ocean to shift to more positive $\delta^{13}\text{C}$ values. The $\delta^{13}\text{C}$ excursions began somewhat before and continued after the deposition of black shales. Moreover, *Tsikos et al.* [2004] show that the stratigraphic position of the peak OAE at different locations, as indicated by the maximum in sedimentary organic carbon (C_{org})

¹Now at National Science Foundation, Arlington, Virginia, USA.

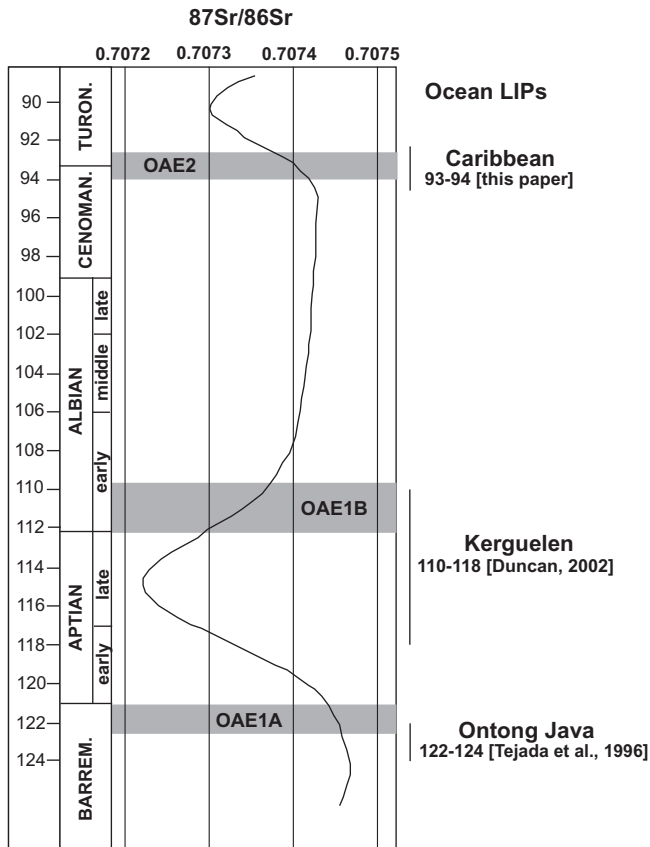


Figure 1. Mid-Cretaceous Sr isotope stratigraphy shows several departures to lower values that have been related to hydrothermal inputs to the oceans. The two decreases pictured here correlate approximately with ocean anoxic events (OAE) 1a and 2, found globally and defined by biostratigraphic and C isotopic data and organic carbon contents. Given the long residence time of Sr in the oceans, abrupt inputs of unradiogenic Sr will be broadened to intervals at least 5 m.y. in duration. The timing of major ocean plateau construction correlates closely with the onset and greatest development of the Sr isotopic lows, and maybe the source for the unradiogenic Sr, rather than pulses or new arrangements of spreading ridges. Figure 1 is amended from *Bralower et al.* [1997] and *Jones and Jenkyns* [2001], with Sr isotopic evolution curve from *Howarth and McArthur* [1997]; timescale is from *Gradstein et al.* [1995] and *Channell et al.* [1995].

contents, varies with respect to the maximum of the $\delta^{13}\text{C}$ excursion. These authors conclude that the slight diachroneity of the OAE was a result of spatial variation in environmental conditions, such as oxygen content related to water depth, circulation and surface productivity.

[5] OAE1a and OAE2 also correlate with a number of well defined Cretaceous extinction events in groups such as the calcareous nannofossils [*Bralower*, 1988; *Erba*, 1994, 2004], radiolarians [*Erbacher et al.*, 1996; *Erbacher and Thurow*, 1997], deep dwelling planktonic and benthic foraminifera [e.g., *Eicher and Worstell*, 1970; *Leckie*, 1989;

Kaiho et al., 1993; *Kaiho and Hasegawa*, 1994; *Kaiho*, 1998; *Premoli Silva and Sliter*, 1999; *Premoli Silva et al.*, 1999; *Leckie et al.*, 2002], and mollusks [e.g., *Kauffman*, 1984; *Kuhnt and Wiedmann*, 1995].

1.1. Global Ocean Anoxic Events

[6] Two processes have been proposed for black shale formation during the Cretaceous: higher productivity and increased organic matter preservation. *Schlanger and Jenkyns* [1976] first suggested that ocean conditions during the mid to Late Cretaceous were favorable for high phytoplankton productivity. Sea level was higher, increasing the area of continental shelves with large influxes of nutrients from rivers, promoting primary productivity. Large fluxes of organic carbon to deep waters could have increased the extent and intensity of the oxygen minimum zone, inducing widespread black shale deposition.

[7] The second process proposed for black shale formation is a global stagnation of ocean circulation. Deep circulation in the young, narrow Atlantic Ocean in the mid and early part of the Late Cretaceous was probably interrupted by volcanic ridges formed by fracture zones and hot spot activity. Warmer average surface temperatures [*Douglas and Savin*, 1975; *Saltzman and Barron*, 1982; *Huber et al.*, 1999, 2002], particularly at high latitudes, led to smaller equator-pole thermal gradients and stronger ocean stratification, both of which inhibited circulation and replenishment of deepwater oxygen. The lower solubility of oxygen in the warmer surface ocean during the Cretaceous resulted in lower concentrations of O_2 throughout the water column, which led to greater preservation of organic carbon, particularly around the expanded oxygen minimum zone.

[8] However, these two explanations do not seem to satisfactorily explain the presence of intermittent OAEs during the mid to Late Cretaceous. For instance, black shale deposits correlate with periods of high species mortality at what would seem to be excellent conditions for marine life [*Kauffman*, 1986; *Larson*, 1991a, 1991b]. Cretaceous OAEs have a very abrupt onset and conclusion, suggesting that some short-period forcing was operating within the longer-term warmer temperatures and higher sea levels, possibly pushing an already poorly oxygenated ocean over a threshold into an anoxic state.

[9] The impact of submarine volcanic eruptions and associated hydrothermal activity is a mechanism for ocean anoxia that has received some recent attention. *Orth et al.* [1993] found high abundances of trace metals in a number of sedimentary sequences deposited about the time of the Cenomanian/Turonian (C/T) boundary, and attributed them to increases in spreading ridge activity. Others have suggested that hydrothermal activity associated with large-scale submarine volcanic events was partly responsible for the decreased levels of O_2 and deposition of black shales [e.g., *Vogt*, 1989; *Erba*, 1994; *Leckie et al.*, 1998, 2002]. More recently, *Sinton and Duncan* [1997], *Larson and Erba* [1999], *Leckie et al.* [2002] and *Erba* [2004] hypothesized that thermally buoyant, metal-rich, eruption-related hydrothermal plumes released during ocean plateau construction may have promoted black shale events.

Table 1. The ^{40}Ar - ^{39}Ar Radiometric Ages for the Caribbean Plateau and Rock Canyon, Colorado^a

Sample	Material	Total Fusion Age $\pm 2\sigma$, ^b Ma	Plateau Age $\pm 2\sigma$, Ma	N	MSWD	Isochron Age $\pm 2\sigma$, Ma	$^{40}\text{Ar}/^{36}\text{Ar}$ Initial $\pm 2\sigma$
Haiti (Dumisseau Formation)							
HA74-25	whole rock	95.12 \pm 1.44	none developed			none developed	
HA76-120	whole rock	94.36 \pm 0.63	none developed			none developed	
HA76-165	whole rock	94.43 \pm 0.66	none developed			none developed	
HA77-28	whole rock	92.16 \pm 0.82	none developed			none developed	
Curacao							
79BE-73	whole rock	88.60 \pm 0.80	92.75 \pm 0.46	4/11	0.87	92.60 \pm 0.86	296.3 \pm 4.2
Western Interior Seaway							
Bentonite (Bridge Creek)	sanidine	94.19 \pm 0.78	94.08 \pm 0.78	5/12	0.79	93.51 \pm 1.10	926 \pm 862

^aAges calculated using biotite monitor FCT-3 (28.04 Ma) and the total decay constant $\lambda = 5.530\text{E-}10/\text{yr}$. N is the number of heating steps (defining plateau/total). MSWD is an *F* statistic that compares the variance within step ages with the variance about the plateau age.

^bMean is 93.96 \pm 0.38 Ma.

1.2. Large Igneous Provinces

[10] Large igneous provinces (LIPs) are massive emplacements of intrusive and extrusive rock erupted over a geologically short period (a few million years) [Coffin and Eldholm, 1994]. These include continental flood basalts, oceanic plateaus and volcanic rifted margins. LIPs do not originate by processes related to those of steady state plate tectonics, such as subduction related volcanic arcs and seafloor spreading, but are proposed to result from surfacing and melting mantle plumes at the beginning stage of hot spot activity [Morgan, 1981; Richards et al., 1989; Duncan and Richards, 1991]. In contrast to the relatively steady state production of crust at seafloor spreading centers, oceanic plateaus are formed by enormous volumes of magma erupted over timescales of 10^5 – 10^6 years [Courtillot and Besse, 1987; Richards et al., 1989]. Eruptions appear to have occurred in short, large-volume pulses lasting days to decades, which is consistent with a flood basalt origin. For brief periods (~ 1 m.y.), submarine oceanic plateau formation probably involved crustal accumulation rates in excess of total mid-ocean ridge rates of production [Duncan and Richards, 1991; Larson, 1991a, 1991b]. During the Cretaceous, a number of these ocean plateaus formed, including the Ontong Java Plateau (early Aptian), the Kerguelen Plateau (late Aptian–early Albian), and the Caribbean Plateau (Cenomanian to Santonian) (Figure 1).

[11] For ocean plateau construction to be related to environmental changes in the ocean observed during OAE2, the timing of volcanic activity must match, within analytical uncertainty, the age of the C/T boundary. Gradstein et al. [1995] estimate the age of the C/T boundary to be 93.5 Ma, based primarily on ^{40}Ar - ^{39}Ar total fusion dating of single sanidine crystals from ash layers from the Western Interior Seaway (WIS) of North America [Obradovich, 1993]. We have confirmed this age with a detailed, ^{40}Ar - ^{39}Ar incremental heating experiment on sanidine separated from ash layer ‘B’ [Elder, 1991], 3 m above the base of the Bridge Creek limestone in the late Cenomanian at Pueblo, Colorado, which provided a plateau age of 94.08 \pm 0.78 Ma (Table 1 and Figure 2).

[12] The ^{40}Ar - ^{39}Ar incremental heating ages from the initial, volumetrically dominant phase of submarine-erupted lava flows from widely distributed parts of the Caribbean

plateau fall in the range 87–95 Ma [Alvarado et al., 1997; Sinton et al., 1998; Hauff et al., 2000]. These are generally low-potassium (tholeiitic), aphyric basalts, which show variable alteration of groundmass to clay and zeolite. Many experiments show disturbed patterns (e.g., Ar loss) and reliable plateau ages are rare because of Ar recoil effects in these fine-grained rocks. Hornblendes separated from pegmatitic rocks intruding submarine lava flows in Colombia have produced acceptable plateaus from 92.55 \pm 1.79 Ma (mean of two) to 89.73 \pm 1.08 Ma (mean of two) [Kerr et al., 2004].

[13] We have selected four, relatively fresh samples from Haiti (Dumisseau Formation [Sen et al., 1988]) and one sample from Curacao (described by Sinton et al. [1998]) for additional ^{40}Ar - ^{39}Ar incremental heating experiments, using the methods described by Duncan [2002]. The Haitian basalts all produced Ar recoil affected age spectra, with step ages decreasing from low- to high-temperature release (Figure 2). However, there is no evidence in low-temperature step ages for significant alteration-induced ^{40}Ar loss or irradiation-induced ^{39}Ar loss. Hence ^{37}Ar and ^{39}Ar isotopes have been redistributed during irradiation, but not lost from the samples, and summing all step compositions should yield reliable total fusion ages. This appears to be a valid conclusion from the tight group of total fusion ages (mean = 93.96 \pm 0.38 Ma). The single sample from Curacao did produce an acceptable plateau age at 92.75 \pm 0.46 Ma, concordant with its isochron age. The weighted mean of the five reliable ages is 93.46 \pm 0.29 Ma, which correlates well with best age estimate for the C/T boundary. Volcanic activity during the main initial phase of Caribbean plateau construction continued until about 87 Ma. It is not yet possible to assign volumes and eruption rates through this period, but we note that other large igneous provinces (e.g., Columbia River, Deccan, and North Atlantic) were built by early, intense intervals of activity, tapering rapidly to intermittent eruptions over several million years.

[14] Sinton and Duncan [1997] proposed that there was a strong link between ocean plateau formation and changes in ocean chemistry, in particular anoxia, during the mid to Late Cretaceous. In their model, heat and metals released during hydrothermal activity associated

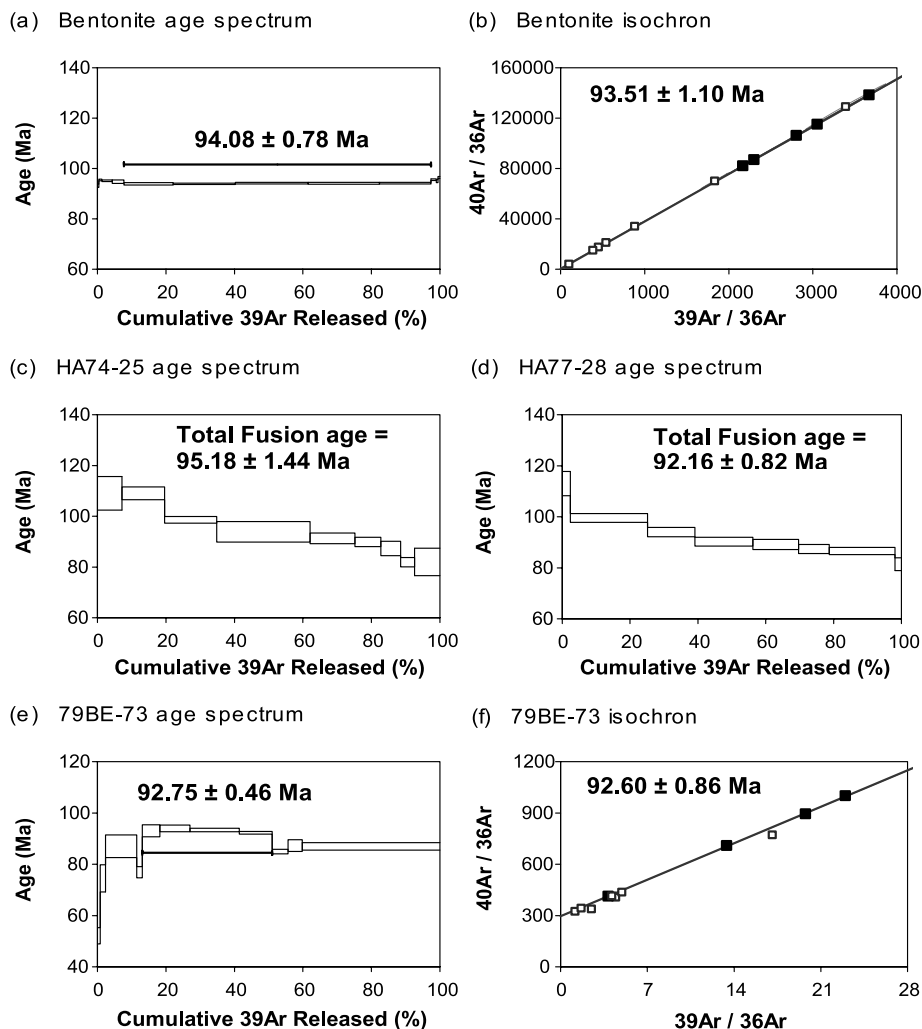


Figure 2. New radiometric ages (^{40}Ar - ^{39}Ar incremental heating method) for (a and b) sanidine separated from a bentonite from the Rock Canyon C/T section (Pueblo, Colorado) and whole rock basalts from (c and d) Haiti and (e and f) Curacao. In age spectrum plots, heating step ages are plotted against proportion of total gas released, resulting in clearly defined “plateaus” of concordant age over multiple, consecutive steps for Figures 2a and 2e but decreasing step age with temperature (^{39}Ar “recoil”) for Figures 2c and 2d. Isochron plots corresponding to the two plateau ages are shown in Figures 2b and 2f.

with single large ocean plateau eruptions had profound effects on the ocean environment, starting with the oxidation of reduced metals and consumption of O_2 in the local water column. Considering that O_2 concentrations in the deep ocean were generally lower during the Cretaceous, this could have been a significant portion of the ocean. The heat released by these enormous lava flows was sufficient to carry metals to the surface ocean [Vogt, 1989]. This large influx of possible nutrients in the form of biolimiting metals (e.g., Fe, Cu, V) likely increased primary production [Coale *et al.*, 1996; Sunda and Huntsman, 1996; Leckie *et al.*, 2002] and possibly led to toxic conditions [e.g., Erickson and Dickson, 1987], both promoting the rain of organic material to the deep ocean and further consumption of O_2 . The combination of oxidation of metals released in hydrothermal plumes, productivity stimulated by nutrients, and

sinking organic material may have periodically had a large enough effect to cause global anoxia.

1.3. Hydrothermal Activity and Oceanic LIPs

[15] Ocean plateaus appear to be the submarine equivalents of continental flood basalt provinces [Sinton *et al.*, 1998] at which volcanic activity occurred as a series of intermittent but large magmatic events, with individual lava flows up to thousands of cubic kilometers in volume [Swanson *et al.*, 1975; Ho and Cashman, 1997]. Considering that ocean lithosphere is thinner and denser than continental crust, even larger volumes of magma could be expected to rise to the Earth’s surface in ocean basins if melting rates were high enough. Therefore it is possible that individual flows from ocean plateau eruptions were much larger (maybe even up to $10,000 \text{ km}^3$ modeled by Sinton and Duncan [1997]).

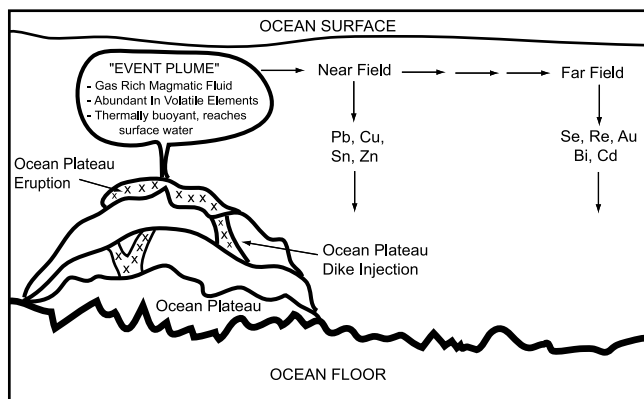


Figure 3. Schematic drawing showing what occurs during an ocean plateau eruption. A large eruption or dike injection releases a gas-rich magmatic fluid abundant in volatile elements. This megaplume has enough heat and energy, and comes from a shallow enough depth, that it reaches the ocean surface and is caught in surface circulation. Metals will then fractionate and precipitate out depending on their reactivity (residence times). Those that precipitate out close to the source are termed “near-field” elements, and those that precipitate out far from the source are termed “far-field” elements.

[16] Warm fluid venting at mid-ocean spreading ridges occurs as steady state hydrothermal plumes associated with the convection of seawater through hot rock [Corliss *et al.*, 1979] and occasional larger releases of warm water triggered by tectonic or volcanic events [Baker *et al.*, 1987; Lupton *et al.*, 1999]. However, neither type of hydrothermal activity produces plumes with enough buoyancy to reach the surface ocean, so nutrients released by volcanic activity at spreading ridges cannot induce higher productivity. Vogt [1989] argued that a hydrothermal plume produced from an eruption of $\sim 15 \text{ km}^3$ would have sufficient energy to bring bottom water to the ocean surface from 3 km deep (typical spreading ridge axial depths). Considering that LIPs could be built from much larger single eruptions (up to $10,000 \text{ km}^3$) at considerably shallower depths ($\sim 1 \text{ km}$), degassed magmatic fluids, mixed with warmed ambient seawater, undoubtedly had enough buoyancy to rise to the surface. These fluids would deliver metals that could be transported rapidly throughout the surface ocean (Figure 3). Such metals would enter into a variety of chemical exchanges (many biologically mediated) and would ultimately be removed from the surface as sinking particles that accumulated as sediments.

[17] An important aspect of the Sinton and Duncan [1997] model is that the chemical exchange of elements to seawater during eruption of large lava flows is controlled by the volatility exchange between basalts and very high temperature, gas-rich magmatic fluids [Rubin, 1997]. The compositions of degassing fluids, and therefore the abundance pattern of elements released to seawater in the form of an eruption event plume, are significantly different from those derived from the solubility-driven exchange between hot water and rock (e.g., typical high-temperature, steady

state hydrothermal vents) [Bowers *et al.*, 1985]. Rubin [1997] estimated that the general predicted element enrichment pattern in a magmatic fluid is as follows: main group elements greater than transition metals greater than alkaline earths similar to alkali metals greater than rare earths and actinides. For marine hydrothermal processes, it is nearly the opposite: alkaline earths similar to alkali metals greater than transition metals greater than rare earths and actinides greater than main group elements. For example, many volatile transition metals and main group metals such as Hg, Bi, Se, Cd, and As are expected to be much more prevalent in degassed effluents (“event plumes”) whereas the concentrations of Fe, Al, Zn, Mn, Ir, the lanthanides, alkali metals and alkaline earth elements are $10\text{--}10^4$ greater in hydrothermal fluids (steady state vents). Therefore these different chemical signatures, recorded in pelagic sediments, could provide a way to distinguish between metal enrichments produced by eruption-related event plumes and those by hydrothermal vents.

1.4. Metal Abundance Anomalies

[18] Orth *et al.* [1993] reported two closely spaced metal abundance peaks just below the C/T boundary from a number of sites in the Western Interior Seaway (WIS) of North America and around the world. These metal anomalies seem to correlate closely to a number of mollusk, planktonic and benthic foraminifera extinctions [Eicher and Worstell, 1970; Hart and Bigg, 1981; Leckie, 1985; Elder, 1987], and the onset of the well-documented positive $\delta^{13}\text{C}$ excursion in the late Cenomanian, and OAE2 which corresponds to globally distributed organic-rich horizons, including the “Bonarelli level” of Italy [e.g., Arthur and Premoli-Silva, 1982] and the “Black Band” of England [e.g., Hart and Bigg, 1981].

[19] Elements that showed enrichment patterns in the work of Orth *et al.* [1993] are Sc, Ti, V, Cr, Mn, Co, Ni, Pt and Au. The authors attribute these metal abundance peaks to new or increased activity in spreading center or hot spot activity in the eastern Pacific basin. However, their suggested source of metals does not explain the sharp onset, brevity and magnitude of these metal abundances. Instead, Sinton and Duncan [1997] proposed that the metal peaks of the C/T boundary are not a result of continuous magmatic activity, but rather of abrupt and distinct hydrothermal “event plumes” released in conjunction with the rapid formation of the Caribbean ocean plateau.

[20] From the relative abundance of these metal anomalies with respect to geographic location, we see that the strongest signals are in the south central and southern regions of the WIS (Figure 4). The concentrations decrease sharply to the north and more gradually to the east and west. Orth *et al.* [1993] attribute this distribution pattern to a source of metals to the south, perhaps from or via the proto-Gulf of Mexico/Caribbean area or far eastern Pacific.

2. Geological Setting

[21] The Rock Canyon Anticline section is located in south central Colorado near Pueblo, Colorado. During the Cretaceous, this location lay in the Western Interior Seaway (WIS), a shallow inland sea that extended across more than

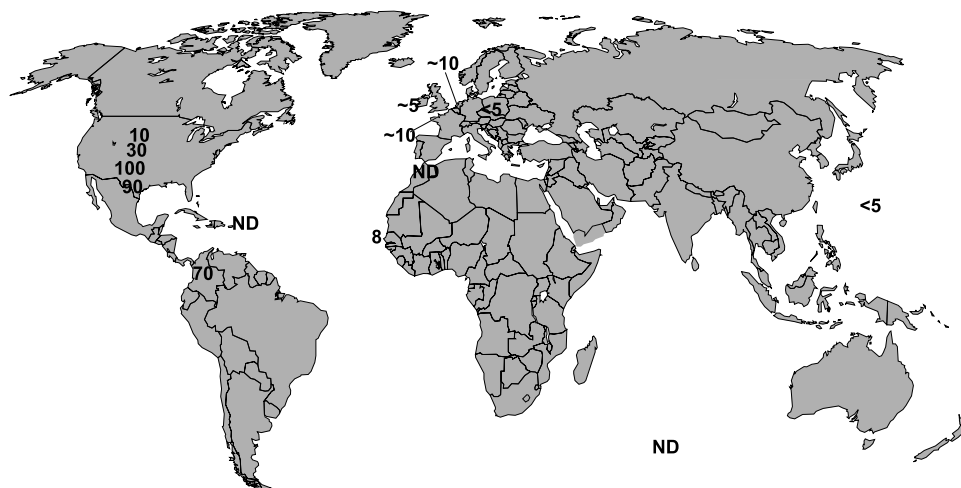


Figure 4. Relative global distributions of elemental anomalies measured by *Orth et al.* [1993] with the site of greatest abundance anomalies assigned a value of 100. ND is anomalies not detected. Strongest signals are in the Western Interior Seaway of the United States and northern Colombia. Intensities drop off sharply to the north and more gradually to the east and west.

30° latitude from the Gulf of Mexico to the Arctic Ocean, with water depths ranging to about 1500 m [e.g., *Kauffman*, 1977; *Hay et al.*, 1993; *Sageman and Arthur*, 1994]. Sedimentation in this area was dominated by a mixture of deposition of pelagic material and siliciclastic material derived from the uplifted fold and thrust basin to the west [Kauffman, 1984]. One of the most studied rock formations of the Cretaceous WIS is the Greenhorn Formation, which was located in the central part of the seaway [e.g., *Pratt et al.*, 1993; *Dean and Arthur*, 1998]. Deposition of this formation (estimated water depths ~200–300 m) began during an interval of rising sea level prior to the peak transgression that occurred in the early Turonian [Sageman and Arthur, 1994].

[22] The Bridge Creek Limestone and Hartland Shale units of the Greenhorn Formation are marked by interbedded, light colored, highly bioturbated limestone and finely laminated dark colored marlstone or calcareous shale. The dark color of the marlstones and shales in the Hartland Shale unit is due to higher concentrations of organic material (total organic carbon (TOC) ~3–5%) whereas the lighter limestones in the Bridge Creek unit contain more carbonate-rich sediments (TOC < 1%, with thin organic-rich, 2–4% layers) [Sageman et al., 1998]. The limestone–shale couplets have been interpreted to reflect climate-driven changes in productivity, clastic dilution and benthic oxygenation [e.g., *Pratt*, 1984; *Barron et al.*, 1985; *Pratt et al.*, 1993].

[23] Molluscan and microfossil biostratigraphy of the Rock Canyon section has been studied in detail. In addition, well-defined lithologic changes, and a number of well-dated bentonite layers [Kauffman et al., 1993; *Obradovich*, 1993] provide excellent time constraints and correlation with other sections in the WIS. The global positive $\delta^{13}\text{C}$ shift (>3‰) in both carbonate and organic carbon fractions, characteristic of OAE2, is also clearly expressed in the Rock Canyon section [Pratt et al., 1993]. This excursion was brought

about by a major shift in the global carbon budget, most likely reflecting the increased burial of isotopically light organic matter ($\delta^{13}\text{C}$ in the range of –20 to –30‰) under anoxic conditions [Scholle and Arthur, 1980]. Sedimentation rates of the Rock Canyon section average around 2.7 cm/k.y. in the Hartland Shale and around 0.9 cm/k.y. in the Bridge Creek Limestone [Meyers et al., 2001].

3. Methods

[24] Sampling at Rock Canyon extended from the uppermost part of the Hartland Shale through to the lower Bridge Creek Limestone, spanning about 8 m below and 6 m above the C/T boundary defined by ammonites [Elder, 1991]. Samples were collected and measured with reference to the base of a prominent, basal limestone, taken as the 0 cm position and correlated to the numbered marker beds of *Cobban and Scott* [1972]. Samples were taken every 30 cm from –4 m to 0 m, every 10 cm from 0 m to 1.5 m, every 2 cm from 1.5 m to 3 m, every 10 cm from 3 m to 4.2 m, and every 50 cm from 4.2 m to 10 m.

[25] Whole rock samples were crushed and powdered, then dissolved in strong acids (hydrofluoric, nitric, and hydrochloric) using a CEM Mars 5 microwave digester. This procedure included a high-heat, high-pressure protocol followed by a sequence of chemical evaporations. Standard reference materials and analytical blanks were prepared according to the same procedure.

[26] Twenty-eight trace and minor element concentrations were determined simultaneously using inductively coupled plasma mass spectrometry (a VG PQ-Excel) and ten major element concentrations were determined using inductively coupled plasma–atomic emission spectrometry (ICP-AES). All elemental concentrations were normalized to Zr. The only significant source of Zr to pelagic sediments is from terrigenous material, thus normalizing to Zr removes the effect of variable terrigenous input to these sediments

Rock Canyon

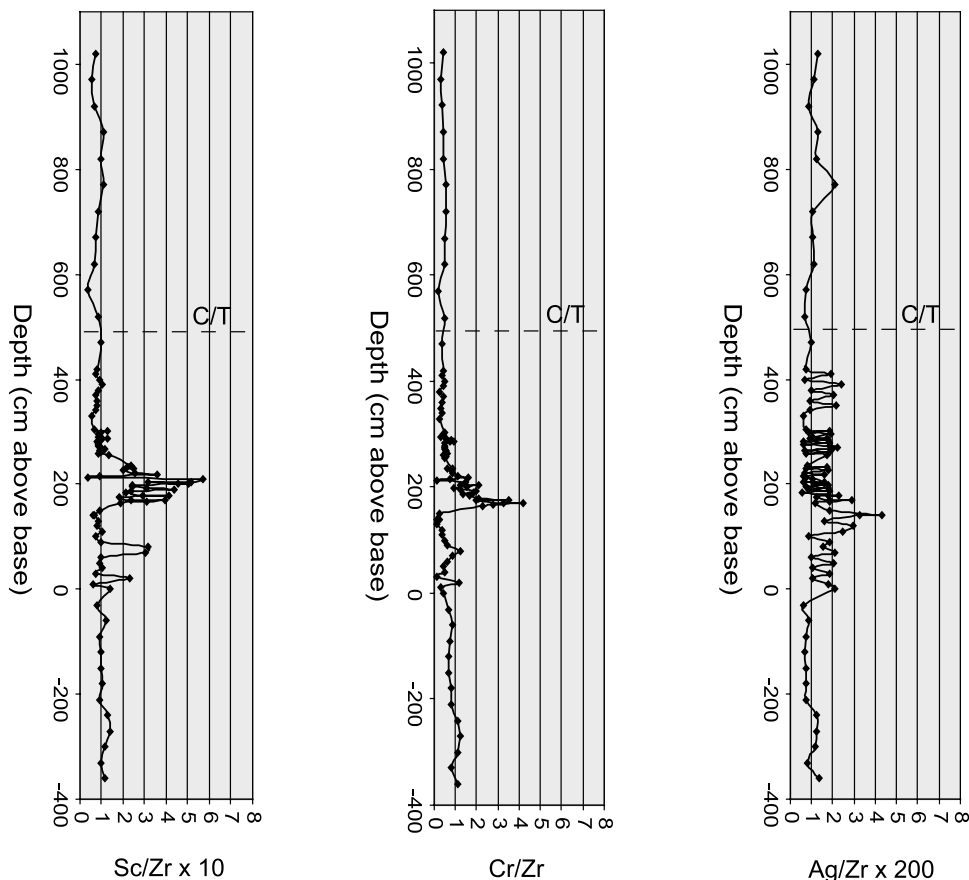


Figure 5. Sc, Cr, and Ag as Zr-normalized metal abundances for the Rock Canyon section, plotted with respect to position above the base of the Bridge Creek Limestone Member, Greenhorn Formation [Sageman *et al.*, 1998]. An interval of high metal abundances can be seen, beginning about 4 m below the Cenomanian/Turonian (C/T) boundary (shown as the dashed line).

[Milnes and Fitzpatrick, 1989]. Zr normalization also corrects for highly variable carbonate contents in the Bridge Creek Limestone.

[27] On the basis of the analysis of blind duplicates and standards the average error for most elements for ICP-MS analyses is about 10% (2σ). However, some elements have slightly higher errors. One group, which includes Sc, V, Ni, Sn, Sb, Cs and Bi, exhibited errors of about 15% and a second, which includes Ag, Au and Se, about 21%. Because of this larger instrumental uncertainty, inferences from this last group of elements should be treated with more caution. The average error for ICP-AES analyses generally ranged from 3 to 8%.

4. Results and Discussion

[28] A 2.5 m interval of Zr-normalized metal abundance anomalies can be seen in the uppermost Cenomanian, lowermost Bridge Creek Limestone between ~ 0 m and 2.5 m (Figure 5). Within this interval are several distinct peaks with much higher abundances. The largest of these

metal abundance peaks spans about 115 cm and is centered at about 2 m. There is a precursor of weaker metal abundances that spans 80 cm centered around the basal limestone (0 m). The upper anomaly is especially well developed in Mn, Ba, Y, Au and Sr, ranging about 8–20 times background levels, and more weakly in Sc, As, Bi, Ag, Na, Cr, Co, Ni, Cu, Cd, Fe, V, Se, W, Pb, Mg and Ti ranging from 3–6 times background levels. The lower anomaly is well developed in Mn, Na, Ba, Cr, Co and Sc, ranging about 5–7 times background levels, but is also seen in Sr, Y, Cu, Ag, W, Ni, Bi, Fe, Se, V, Au, As, Pb, Mg, Ti and Cd ranging about 2–4 times background levels.

4.1. Character of Metal Abundance Anomalies

[29] If event plume activity occurred near the time of the C/T boundary, an increase in trace metals in surface ocean waters should be reflected in the pelagic ocean sediments accumulating at these times. Certain metals specifically associated with event plume activity give us a diagnostic suite of elements to look for in these sediments. According to Rubin [1997], highly volatile elements, such as B, Bi, Cd,

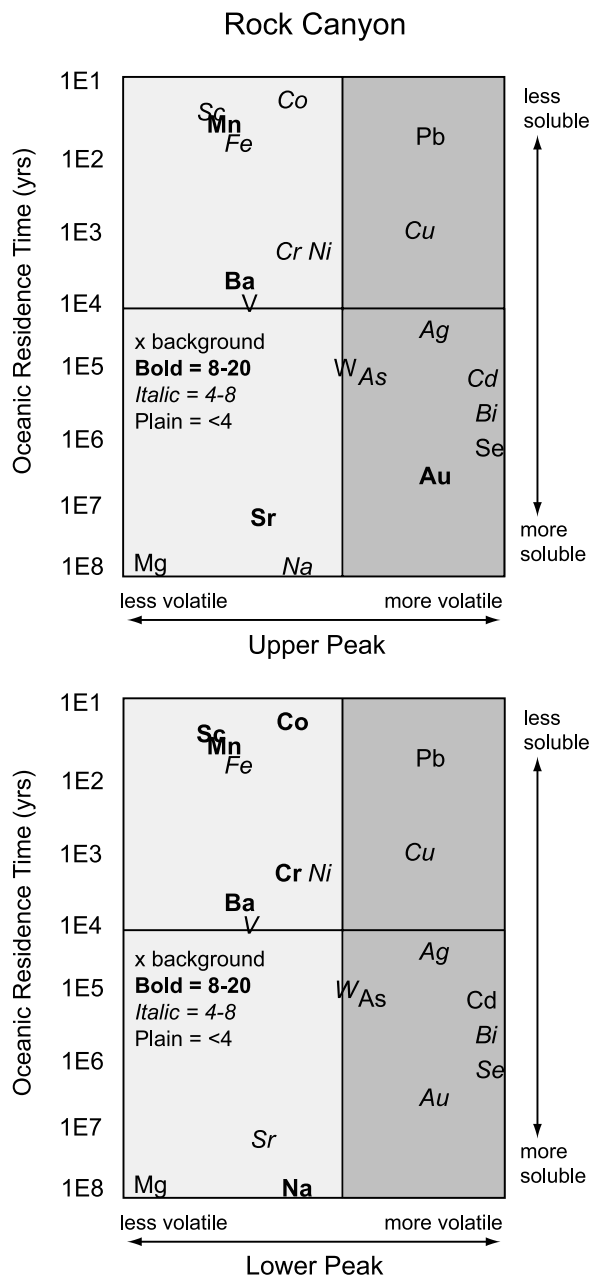


Figure 6. Elements enriched in pelagic sediments may be distinguished by origin and distance from source by considering their relative volatility and ocean residence time, according to a matrix developed by Rubin [1997]. Elements in lightly shaded boxes (left) tend to be more enriched in steady state seafloor-spreading hydrothermal activity whereas elements in more heavily shaded boxes (right) tend to be more enriched in eruption-related plumes. Elemental abundance anomalies, normalized to Zr, are presented for the upper and lower peaks at the Rock Canyon C/T boundary section.

Se, Hg, Ag, Pb, Au, Cu, As, Zn, Tl, In, Re, Sn and Mo, are concentrated in magmatically degassed fluids released by eruptions. Elements that are less volatile, such as Fe, Mn, Ba, V, Sr, Sc, Co, Cr, Ni and Rb would more likely be found in higher concentrations in water/rock exchange reactions of typical steady state hydrothermal vents. Elemental abundance patterns at Rock Canyon reveal an interval of increased abundances in both the nonvolatile and volatile elements (Figure 5). The presence of these anomalies indicates that concentrations of metals in the ocean, or at least at this site, were increased by some mechanism other than influx of terrigenous sediment, possibly the release of magmatic fluids in event plumes. The variation in percent TOC does not correlate with the position of the metal peaks, indicating that redox conditions at the sediment-water interface or increased scavenging of metals by sinking organic matter cannot explain the metal abundance anomalies. Percent TOC in the Hartland Shale is generally higher (3–5% [Sageman *et al.*, 1998]), but no metal abundance anomalies occur in the upper 4 m of this unit, so scavenging by sinking organic matter has not been a significant source of metals. We interpret the anomalies at Rock Canyon, in both the nonvolatile and volatile elements, to indicate that this area was proximal to a region of elevated magmatic degassing and increased hydrothermal venting.

[30] An important aspect of many trace metals is that once they enter the ocean environment, they become biologically active (metabolic processes) and chemically reactive (inorganic reactions), and are removed from seawater by sinking organic matter (scavenging). Depending on how reactive they are, some will be scavenged very quickly whereas others will remain in ocean water much longer. An element’s reactivity can be represented by its mean oceanic residence time (total mass dissolved in oceans/rate of supply or removal). The behavior of elements in the stronger, upper interval of metal abundance anomalies from Rock Canyon can be evaluated in a plot of volatility versus residence time (Figure 6). Elements that are less volatile and have shorter residence times are generally more enriched (abundances 8–20 times background levels) compared with elements that are more volatile and/or have longer residence times, ranging about 4–8 times background levels. Enrichment in the less volatile elements indicates that the Rock Canyon site reflects water/rock exchange hydrothermal activity. This hydrothermal activity occurred on an intermittent timescale rather than the “steady state” activity associated with mid-ocean ridge spreading centers. The upper abundance peak interval also shows enrichment in elements that are more volatile with a wide range of residence times. These elements are present at about 2 (e.g., Pb) to 6 (e.g., Cu) times background levels. The presence of the more volatile elements suggests that Rock Canyon records effects of magmatic degassing as well. The lower (precursor) abundance anomaly peak from Rock Canyon also follows this same general abundance pattern: the less volatile, more reactive elements ranging about 7–18 times above background levels and the more volatile, less reactive elements ranging about 2–6 times above background levels.

[31] These volatility versus residence time comparisons, for both the upper and lower abundance peaks, seem to be consistent with the location of Rock Canyon relative to the suspected source of event plumes. Assuming the source of event plumes was the Caribbean plateau (over the Galapagos hot spot at 93–94 Ma), the Rock Canyon was around 5000 km from this source (distance based on reconstructed plate position to ~ 90 Ma from *Wignall* [1994]). Thus it is not surprising to observe enrichments in elements found in both water/rock hydrothermal exchange activity and magmatic degassing, but also to see a change in element enrichment factors based on residence time. That is, metal anomalies are more pronounced in those elements that are more reactive, termed near-field elements, compared to those elements that are less reactive, termed far-field elements. Eruptions on ocean plateaus could have been up to thousands of km³ in volume, producing enough water/rock hydrothermal activity and magmatic degassing effluents to affect a site at a distance of 5000 km.

[32] It should be noted that the elemental abundance anomalies at Rock Canyon do not exactly follow the volatility versus residence time predicted pattern [*Rubin*, 1997]. The Rock Canyon section was deposited in 200–300 m water depths; depth-dependent scavenging may have an effect on results otherwise dependent on distance. The predicted pattern is also based on present ocean chemistry, and Cretaceous ocean residence times may have been somewhat different for some elements. For example, if ocean waters became dysoxic/anoxic, Fe and Mn would become significantly more soluble, increasing their residence times.

[33] Also, some of the major and minor element abundances with large anomalies, such as Na, Mg, Sr and Ca, are major constituents of seawater and event plumes would probably not significantly change their concentration in seawater. Therefore it seems likely that another source in addition to increased hydrothermalism is responsible for higher concentrations in seawater of these elements at this time. One possible explanation is that excess CO₂ from volcanism may have decreased the pH of rainwater, enhanced continental weathering and increased the elemental concentrations in river water.

4.2. Position of Metal Anomalies, Carbon Isotopes, and Species Mortality

[34] The onset of OAE2 is recognized globally by the shift toward more positive $\delta^{13}\text{C}$ values, although the timing of peak anoxia apparently differed slightly from place to place in the oceans [*Tsikos et al.*, 2004]. The usual explanation for this global change is that ¹²C-enriched marine organic matter was removed from the ocean-atmosphere reservoir (i.e., buried) [*Jenkyns*, 1980; *Arthur et al.*, 1987]. The diminished return of light carbon, due to low levels of benthic oxygen in expanding oxygen minimum zones [*Arthur et al.*, 1987; *Schlanger et al.*, 1987; *Pratt et al.*, 1993], left the ocean enriched in heavy carbon [*Scholle and Arthur*, 1980] and produced the positive $\delta^{13}\text{C}$ values. As this process continued through the duration of the ocean anoxic event, ocean $\delta^{13}\text{C}$ values became increasingly more

positive. The conclusion of OAE2 is recognized by the shift in the carbon isotope curve back to more negative (i.e., background) $\delta^{13}\text{C}$ values. This shift indicates that light organic matter was returned to the ocean, because of weathering of exposed rocks on land and increased oxygenation of deep water and greater remineralization of organic matter. Bulk sedimentation rates for the Rock Canyon section have been determined from evolutive harmonic analysis and stratigraphic modeling by *Meyers et al.* [2001]. On the basis of their average sedimentation rates, and with reference to the global $\delta^{13}\text{C}$ profile, OAE2 lasted about 600 kyr.

[35] To determine the relationship between the metal anomalies in the Rock Canyon section and the onset and duration of the globally variable OAE2 events, we examined their timing relative to the carbon isotope curve ($\delta^{13}\text{C}_{\text{org}}$ [*Pratt*, 1985; *Bowman and Bralower*, 2005], see Figure 7). All time estimates are based on average sedimentation rates from *Meyers et al.* [2001]. The lower weaker interval (0–40 cm, lower *S. gracile* biozone) of metal abundance anomalies correlates with the beginning of the positive $\delta^{13}\text{C}_{\text{org}}$ excursion, at the onset of OAE2. In the better resolved profile [*Bowman and Bralower*, 2005], $\delta^{13}\text{C}_{\text{org}}$ values return briefly to background ($\sim -27\text{‰}$, C_{org}) before climbing again to the long positive interval. This precursor spike corresponds possibly to an early phase of volcanic activity separated from the main period of volcanic construction, or, as *Bowman and Bralower* [2005] propose, the brief negative shift reflects oxidation of organic matter in outcrop samples. The upper, stronger interval (160–220 cm, uppermost *S. gracile* and *N. juddii* biozones) of metal abundance anomalies occurs at the onset of the plateau in values in the Rock Canyon $\delta^{13}\text{C}_{\text{org}}$ curve (event C as denoted by *Pratt* [1985]). Both metal anomalies lasted about 120 kyr, which suggests that volcanic activity occurred over a similar time period. This timing is consistent with the speculated eruption history of ocean plateaus, which is that magmatism occurs in short, large volume pulses erupting in periods of days to decades, over a total duration of 10^5 – 10^6 years. The stratigraphic position of these metal anomalies, the lower peak at the onset of the $\delta^{13}\text{C}_{\text{org}}$ excursion and the upper peak close to the C/T boundary, at the plateau of the $\delta^{13}\text{C}_{\text{org}}$ excursion, gives a good indication of the timing of events with respect to the global OAE2.

[36] However, C_{org} contents are more revealing of the timing of local OAE events, which have been shown to vary stratigraphically, depending on location, with respect to the $\delta^{13}\text{C}_{\text{org}}$ excursion [*Tsikos et al.*, 2004]. The lower metal peak lies close to a minor peak in C_{org} [*Sageman et al.*, 1998], possibly the onset of the OAE in the WIS; the upper metal peak slightly precedes the maximum in C_{org} [*Sageman et al.*, 1998; *Bowman and Bralower*, 2005]. In Italy the maximum C_{org} interval (Bonarelli level) coincides with the rise in $\delta^{13}\text{C}_{\text{org}}$, therefore approximately coincident with the stratigraphic position of the maximum metal peak. Thus the phasing of the Caribbean plateau hydrothermal activity appears to be similar to the OAE in the WIS, but is slightly diachronous with the event in the

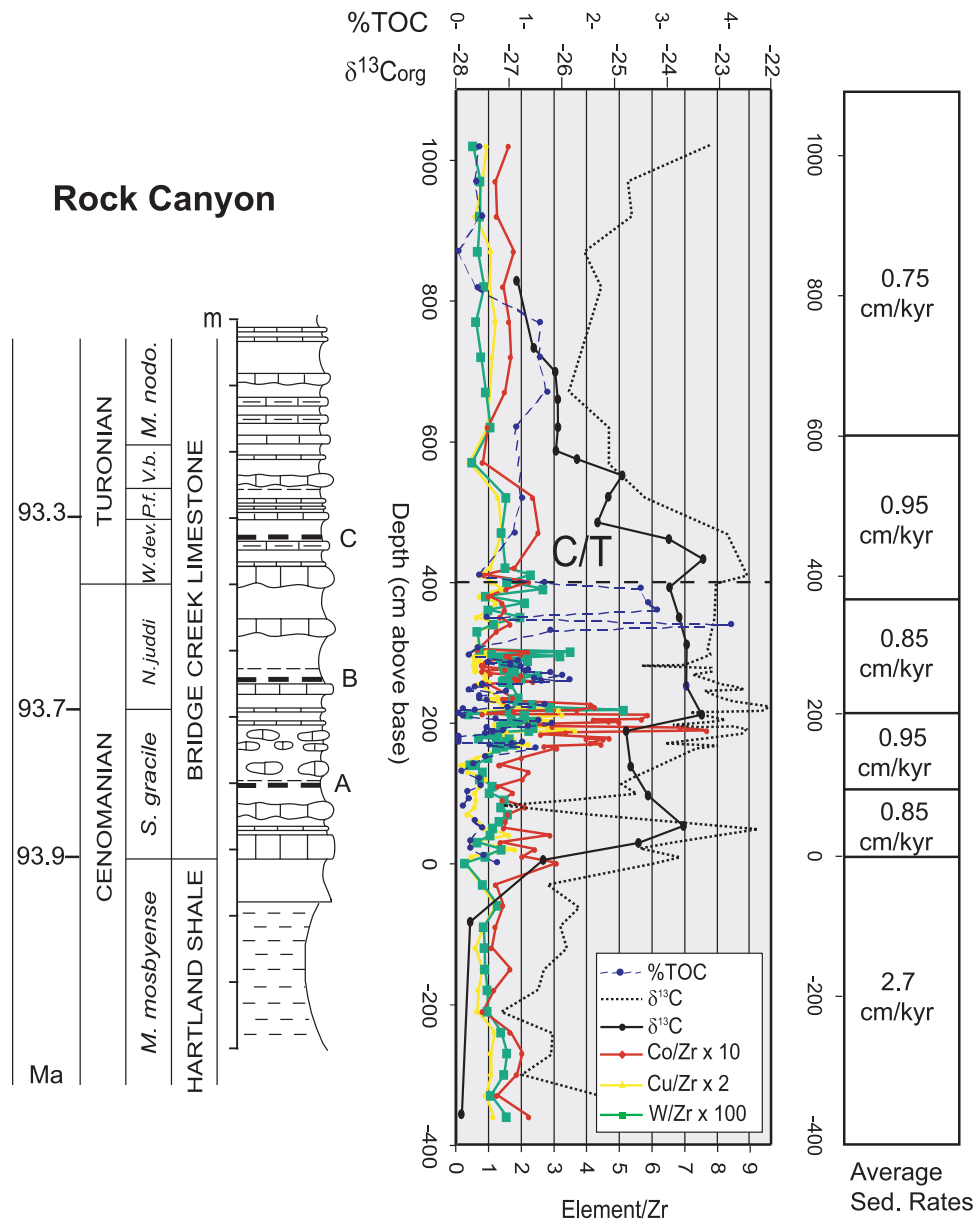


Figure 7. Position of the Rock Canyon metal abundance anomalies with respect to the carbon isotopic curve. Carbon data ($\delta^{13}C_{org}$) are from Pratt et al. [1993] (solid line) and from T. J. Bralower (unpublished data, 2003) (short-dashed line). Percent TOC data (long-dashed line) are from Bowman and Bralower [2005]. Timescale is from Kauffman et al. [1993], drafted section is from Elder and Kirkland [1985], and sedimentation rates are from Meyers et al. [2001]. C/T boundary is shown as horizontal dashed line; areas labeled A, B and C are prominent bentonite layers.

Tethys. We speculate that the proximal location of the WIS with respect to the Caribbean resulted in more direct forcing of anoxia by hydrothermal environmental variables controlling the exact timing of the OAE. More metal stratigraphies are required to clarify the relationship of the timing of peak hydrothermal activity and the anoxic event at different locations.

[37] Another important relationship is the position of the metal anomalies with respect to species mortality. The

release of high abundances of trace metals to the ocean surface has the potential to increase primary productivity and/or produce mass mortality from toxic metal concentrations. Therefore, looking at the biostratigraphic data can give yet another indication of the order of events during this period. It has been documented that major species perturbations, particularly in radiolaria, calcareous nannoplankton [Bralower, 1988; Erbacher and Thurow, 1997; Premoli Silva et al., 1999] and deeper dwelling

planktic foraminifera, occurred during the main OAE2 event and have been attributed to changes in temperature, water column structure and the expansion of the oxygen minimum zone [Leckie, 1985, 1989]. However, more noteworthy is a study conducted by Leckie *et al.* [1998] of planktonic and benthic foraminiferal assemblages in rocks from several sections of the southwestern WIS, including the Rock Canyon section. The interval of metal anomalies determined in this section falls in the same position as an interval with major changes in the assemblages of planktic and benthic foraminifera and pulses of extinctions in mollusks, about 2 m below the C/T boundary [Elder, 1991; Leckie *et al.*, 1998].

[38] According to Leckie *et al.* [2002], changing nutrient availability and water column stratification, possibly related to elevated rates of hydrothermal activity, were likely the major factors responsible for high species turnover during OAE2. Increased rates of speciation and extinction may be a result of higher fluxes of biolimiting trace metals, stimulating production and opening new niches, or leading to toxicity. Also, excess CO₂ from volcanism may have resulted in increased continental weathering, leading to increased runoff of nutrients, stimulating production and species turnover. Conversely, excess CO₂ may have lowered seawater pH and reduced alkalinity, stressing calcareous plankton and possibly leading to extinctions of certain taxa [Leckie *et al.*, 2002]. An increased supply of nutrients may in fact have had an indirect negative effect on some species. Habitat expansion of previously nutrient-limited organisms may have resulted in major changes to ecosystems. Erba [1994] suggested this as a partial cause for the early Aptian “nannoconid crisis,” in which a group of heavily calcified calcareous nannoplankton experienced dramatic thinning of tests and a drop in abundance, and the same may have been true in producing the demise of species around OAE2.

5. Summary and Conclusions

[39] Major, minor and trace element abundances were measured in a C/T boundary section from Rock Canyon, Pueblo, Colorado. The C/T boundary of the Late Cretaceous correlates with the end of OAE2 and with the massive volcanism that built the Caribbean ocean plateau, starting at around 93–94 Ma. Sinton and Duncan [1997] suggest that these events are related because of their temporal coincidence. In particular, they propose that metal-rich, eruption-related hydrothermal event plumes accompanying ocean plateau construction may have pushed the ocean temporarily into anoxia. If this hypothesis is true, high metal abundances, marking the presence of ocean plateau hydrothermal plumes should be present in sedimentary sections bracketing the C/T boundary. The stratigraphic position of metal abundance anomalies indicates the timing of plumes with respect to the onset of anoxia and other linked biogeochemical responses.

[40] Trace, minor and major element analyses have revealed an interval with two distinct abundance peaks. The lower, weaker anomaly, especially well developed in

Mn, Ba, Y, Au and Sr, lies about 4 m below the C/T boundary and the upper, stronger anomaly, well developed in Mn, Na, Ba, Cr, Co and Sc, lies about 2 m below the C/T boundary at the Rock Canyon section. The two anomalous intervals show increased abundances in both the volatile and nonvolatile elements, suggesting this site may have received effluents from both magmatic degassing and hydrothermal water/rock exchange. Both metal-rich intervals are more abundant in the less volatile, more reactive elements, such as Sc, Co, and Mn and Fe, and somewhat less abundant in the more volatile, less reactive elements such as Se, Cd, W, Au and Bi. Assuming the source of event plume metals was the Caribbean plateau, the Rock Canyon is reasonably proximal and, therefore, it is expected to be rich in a wide range of near-field and far-field elements.

[41] The lower peak in metal abundances occurs at the beginning of OAE2 in the WIS, as defined by the initial increase in $\delta^{13}\text{C}_{\text{org}}$ values and C_{org} contents, and the upper peak occurs slightly earlier than the peak of OAE2, at the beginning of the plateau of maximum $\delta^{13}\text{C}_{\text{org}}$ values. High, but variable C_{org} contents occur above the metal abundances, within the plateau of maximum $\delta^{13}\text{C}_{\text{org}}$ values. In Italy, however, the maximum C_{org} contents occur earlier, coincident with the rise in $\delta^{13}\text{C}_{\text{org}}$ at the beginning of OAE2 [Tsikos *et al.*, 2004], and at the same position as metal abundances (S. Turgeon, personal communication, 2003). The diachronous occurrence of maximum C_{org} contents with respect to $\delta^{13}\text{C}_{\text{org}}$ worldwide indicates a spatial variation in environmental conditions, such as oxygen content related to water depth, circulation and surface productivity.

[42] These observations suggest that metal-rich, hydrothermal plumes, probably triggered by massive volcanic eruptions on the Caribbean plateau, lead to productivity events. The coincidence of the metal abundances with the rise in $\delta^{13}\text{C}$ values is consistent with the idea that metals stimulated enough phytoplankton growth and burial of organic matter in the deep ocean to temporarily change the C isotopic composition of seawater. The synchronicity of the metal abundances and high rates of speciation and extinction in foraminifera, calcareous nannofossils, radiolarians and mollusks, as reported by Leckie *et al.* [2002], supports the argument that event plumes carried biolimiting and/or toxic concentrations of metals into the ocean. Increased productivity resulted in an increasing supply of organic carbon to the deep ocean, thus exhausting oxygen supplies and bringing about the demise of benthic species. The collapse of planktic species was most likely brought about by the stress induced by major environmental perturbations, shrinking or loss of ecological habitats, increased predation, increased pCO₂ and river runoff, and possible metal toxicity [Erba, 1994; Leckie *et al.*, 2002]. The onset of OAE2 was also accompanied by a rapid increase in intermediate water depth temperatures, to nearly 20°C, based on data from Blake Nose in the western North Atlantic [Huber *et al.*, 1999]. Such an abrupt warming event may have reduced upper water column stratification leading to the observed evolutionary turnover of plankton [Leckie *et al.*, 2002].

[43] To further determine a connection between formation of the Caribbean plateau and OAE2, it will be important to investigate other pelagic sediment records for signs of submarine volcanic activity and the variation in the patterns and intensities of trace metal abundance anomalies relative to the proposed source of metals (the Caribbean plateau). In addition to the Rock Canyon section, we are determining trace element abundances for a set of globally distributed sections to see if changes in metal patterns and metal abundances are consistent with modeled Late Cretaceous

circulation and with Rubin's [1997] general predicted element enrichment pattern based on element volatility and residence times.

[44] **Acknowledgments.** L.J.S. and R.A.D. thank the W. M. Keck Collaboratory at Oregon State University for use of the ICP-MS and ICP-AES. Thanks to A. Bowman for the use of samples from the Rock Canyon section. This research was funded by the Petroleum Research Fund of the American Chemical Society to R.A.D. and NSF OCE 0084032 (Biocomplexity: The Evolution and the Radiation of Eucaryotic Phytoplankton Taxa (EREUPT)) to T.J.B. We thank Mark Leckie and Elisabetta Erba for reviews that improved this paper.

References

- Alvarado, G. E., P. Denyer, and C. W. Sinton (1997), The 89 Ma Tortugal komatiitic suite, Costa Rica: Implications for a common origin of the Caribbean and eastern Pacific region from a mantle plume, *Geology*, **25**, 439–442.
- Arthur, M. A., and I. Premoli-Silva (1982), Development of widespread organic carbon-rich strata in the Mediterranean Tethys, in *Nature and Origin of Cretaceous Carbon-Rich Facies*, edited by S. O. Schlanger and M. B. Cita, pp. 7–54, Elsevier, New York.
- Arthur, M. A., S. O. Schlanger, and H. C. Jenkyns (1987), The Cenomanian-Turonian ocean anoxic event II, paleoceanographic controls on organic matter production and preservation, in *Marine Petroleum Source Rocks*, edited by J. Brooks and A. Fleet, *Geol. Soc. Spec. Publ. London*, **24**, 399–418.
- Arthur, M. A., H. C. Jenkyns, H. J. Brumsack, and S. O. Schlanger (1990), Stratigraphy, geochemistry, and paleoceanography of organic carbon-rich Cretaceous sequences, in *Cretaceous Resources, Events and Rhythms*, edited by R. N. Ginsburg and B. Beaudoin, pp. 75–119, Springer, New York.
- Baker, E. T., G. J. Massoth, and R. A. Feely (1987), Cataclysmic hydrothermal venting on the Juan de Fuca Ridge, *Nature*, **329**, 149–151.
- Barron, E. J., M. A. Arthur, and E. G. Kauffman (1985), Cretaceous rhythmic bedding sequences: A plausible link between orbital variations and climate, *Earth Planet. Sci. Lett.*, **72**, 327–340.
- Bowers, T. S., K. L. Von Damm, and J. M. Edmond (1985), Chemical evolution of mid-ocean ridge hot springs, *Geochim. Cosmochim. Acta*, **49**, 2239–2252.
- Bowman, A. R., and T. J. Bralower (2005), Paleoceanographic significance of high-resolution carbon isotope records across the Cenomanian-Turonian boundary in the western interior and New Jersey coastal plain, USA, *Mar. Geol.*, **217**, 305–321.
- Bralower, T. J. (1988), Calcareous nannofossil biostratigraphy and assemblages of the Cenomanian-Turonian boundary interval: Implications for the origin and timing of oceanic anoxia, *Paleoceanography*, **3**, 275–316.
- Bralower, T. J., P. D. Fullagar, C. K. Paull, G. S. Dwyer, and R. M. Leckie (1997), Mid-Cretaceous strontium-isotope stratigraphy of deep-sea sections, *Geol. Soc. Am. Bull.*, **109**, 1421–1442.
- Channell, J. E. T., E. Erba, M. Nakanishi, and K. Tamaki (1995), Late Jurassic-Early Cretaceous time scales and oceanic magnetic anomaly block models, in *Geochronology: Time Scales and Global Stratigraphic Correlation*, edited by W. A. Berggren et al., *Spec. Publ. SEPM Soc. Sediment. Geol.*, **54**, 51–63.
- Coale, K. H., et al. (1996), A massive phytoplankton bloom induced by an ecosystem-scale iron fertilization experiment in the equatorial Pacific Ocean, *Nature*, **383**, 495–501.
- Cobban, W. A., and G. R. Scott (1972), Stratigraphy and ammonite fauna of the Graneros Shale and Greenhorn Limestone near Pueblo, Colorado, *U.S. Geol. Surv. Prof. Pap.*, **P-0645**, 108 pp.
- Coffin, M. F., and O. Eldholm (1994), Large igneous provinces: Crustal structure, dimensions and external consequences, *Rev. Geophys.*, **32**, 1–36.
- Corliss, J. B., et al. (1979), Submarine thermal springs on the Galapagos Rift, *Science*, **203**, 1073–1083.
- Courtillot, V., and J. Besse (1987), Magnetic reversals, polar wander, and core-mantle coupling, *Science*, **237**, 1140–1147.
- Dean, W. E., and M. A. Arthur (1998), Cretaceous Western Interior Seaway drilling project: An overview, in *Stratigraphy and Paleoenvironments of the Cretaceous Western Interior Seaway, USA, Concepts in Sedimentol. Paleontol.*, vol. 6, edited by W. E. Dean and M. A. Arthur, pp. 1–10, Soc. of Sediment. Geol., Tulsa, Okla.
- Douglas, R. G., and S. M. Savin (1975), Oxygen and carbon isotope analyses of Tertiary and Cretaceous microfossils from Shatsky Rise and other sites in the North Pacific Ocean, *Initial Rep. Deep Sea Drill. Proj.*, **32**, 509–520.
- Duncan, R. A. (2002), A time frame for construction of the Kerguelen Plateau and Broken Ridge, *J. Petrol.*, **4**, 1109–1119.
- Duncan, R. A., and M. A. Richards (1991), Hot-spots, mantle plumes, flood basalts, and true polar wander, *Rev. Geophys.*, **29**, 483–501.
- Eicher, D. L., and P. Worstell (1970), Cenomanian and Turonian foraminifera from the Great Plains, United States, *Micropaleontol.*, **16**, 269–324.
- Elder, W. P. (1987), The paleoecology of the Cenomanian-Turonian (Cretaceous) stage boundary extinctions at Black Mesa, Arizona, *Palaios*, **2**, 24–40.
- Elder, W. P. (1991), Molluscan paleoecology and sedimentation patterns of the Cenomanian-Turonian extinction interval on the southern Colorado Plateau region, edited by J. D. Nations and J. G. Eaton, in *Stratigraphy, Depositional Environments, and Sedimentary Tectonics of the Western Margin, Cretaceous Western Interior Seaway, Spec. Pap. Geol. Soc. Am.*, **260**, 113–137.
- Elder, W. P., and J. I. Kirkland (1985), Stratigraphy and depositional environments of the Bridge Creek Limestone Member of the Greenhorn Limestone at Rock Canyon Anticline near Pueblo, Colorado, in *Fine-Grained Deposits and Biofacies of the Cretaceous Western Interior Seaway: Evidence of Cyclic Sedimentary Processes*, edited by L. M. Pratt, E. G. Kauffman, and F. B. Zelt, *Field Trip Guideb.*, **4**, pp. 22–134, Soc. of Sediment. Geol., Tulsa, Okla.
- Erba, E. (1994), Nannofossils and superplumes: The early Aptian “nannoconid crisis”, *Paleoceanography*, **9**, 483–501.
- Erba, E. (2004), Calcareous nannofossils and Mesozoic oceanic anoxic events, *Mar. Micropaleontol.*, **52**, 85–106.
- Erbacher, J., and J. Thurow (1997), Influence of oceanic anoxic events on the evolution of mid-Cretaceous radiolaria in the North Atlantic and western Tethys, *Mar. Micropaleontol.*, **30**, 139–158.
- Erbacher, J., J. Thurow, and R. Littke (1996), Evolution patterns of radiolaria and organic matter variations: A new approach to identify sea level changes in mid-Cretaceous pelagic environments, *Geology*, **24**, 499–502.
- Erickson, D. J., III, and S. M. Dickson (1987), Global trace-element biogeochemistry at the K/T boundary: Oceanic and biotic response to a hypothetical meteorite impact, *Geology*, **15**, 1014–1017.
- Gradstein, F. M., F. P. Agterberg, J. G. Ogg, J. Hardenbol, P. van Veen, J. Thierry, and Z. Huang (1995), A Triassic, Jurassic and Cretaceous time scale, in *Geochronology: Time Scales and Global Stratigraphic Correlation*, edited by W. A. Berggren et al., *Spec. Publ. SEPM Soc. Sediment. Geol.*, **5**, 95–126.
- Hart, M. B., and P. J. Bigg (1981), Anoxic events in the Late Cretaceous chalk seas of north-west Europe, in *Microfossils of Recent and Fossil Shelf Sea*, edited by J. W. Neale and M. D. Brasier, pp. 171–185, Ellis Horwood, Chichester, U. K.
- Hauff, F., K. Hoernle, P. van den Bogaard, G. E. Alvarado, and C. D. Garbe-Schonberg (2000), Age and geochemistry of basaltic complexes in western Costa Rica: Contributions to the geotectonic evolution of Central America, *Geochim. Geophys. Geosyst.*, **1**, doi:10.1029/1999GC000020.
- Hay, W. W., D. L. Eicher, and R. Diner (1993), Physical oceanography and water masses in the Cretaceous Western Interior Seaway, in *Evolution of the Western Interior Basin*, edited by W. G. E. Caldwell and E. G. Kauffman, *Geol. Assoc. Can. Spec. Pap.*, **39**, 297–318.

- Ho, A., and K. Cashman (1997), Temperature constraints on the Ginkgo Flow of the Columbia River Basalt Group, *Geology*, 25, 403–406.
- Howarth, R. J., and J. M. McArthur (1997), Statistics for strontium isotope stratigraphy: A robust LOWESS fit to the marine Sr-isotope curve for 0 to 206 Ma, with look-up table for derivation of numeric age, *J. Geol.*, 105, 441–456.
- Huber, B. T., R. M. Leckie, R. D. Norris, T. J. Bralower, and E. CoBabe (1999), Foraminiferal assemblage and stable isotopic change across the Cenomanian-Turonian boundary in the subtropical North Atlantic, *J. Foraminiferal Res.*, 29, 392–417.
- Huber, B. T., R. D. Norris, and K. G. MacLeod (2002), Deep-sea paleotemperature record of extreme warmth during the Cretaceous, *Geology*, 30, 123–126.
- Ingram, B. L., R. Coccioni, A. Montanari, and F. M. Richter (1994), Strontium isotopic composition of mid-Cretaceous seawater, *Science*, 264, 546–550.
- Jenkyns, H. C. (1980), Cretaceous anoxic events: From continents to oceans, *J. Geol. Soc. London*, 137, 137–188.
- Jones, C. E., and H. C. Jenkyns (2001), Seawater strontium isotopes, oceanic anoxic events, and seafloor hydrothermal activity in the Jurassic and Cretaceous, *Am. J. Sci.*, 301, 112–149.
- Jones, C. E., H. C. Jenkyns, A. L. Coe, and S. P. Hesselbo (1994), Strontium isotopic variations in Jurassic and Cretaceous seawater, *Geochim. Cosmochim. Acta*, 58, 3061–3074.
- Kaiho, K. (1998), Phylogeny of deep-sea calcareous trochospiral benthic foraminifera: Evolution and diversification, *Micropaleontology*, 44, 291–311.
- Kaiho, K., and T. Hasegawa (1994), Cenomanian benthic foraminiferal extinctions and dysoxic events in the northwestern Pacific Ocean margin, *Palaeogeogr. Palaeoclimatol. Palaeoecol.*, 111, 29–43.
- Kaiho, K., O. Fujiwara, and I. Motoyama (1993), Mid-Cretaceous faunal turnover of intermediate water benthic foraminifera in the northwestern Pacific Ocean margin, *Micropaleontology*, 23, 13–49.
- Kauffman, E. G. (1977), Geological and biological overview: Western interior Cretaceous basin, *Mt. Geol.*, 14, 75–100.
- Kauffman, E. G. (1984), Paleobiogeography and evolutionary response dynamic in the Cretaceous Western Interior Seaway of North America, in *Jurassic-Cretaceous Biochronology and Paleogeography of North America*, edited by G. E. G. Westermann, *Geol. Assoc. Can. Spec. Pap.*, 27, 273–306.
- Kauffman, E. G. (1986), High-resolution event stratigraphy: Regional and global Cretaceous bio-events, in *Global Bio-Events: A Critical Approach*, edited by O. H. Walliser, pp. 279–335, Springer, New York.
- Kauffman, E. G., B. B. Sageman, W. P. Elder, J. I. Kirkland, and T. Villamil (1993), Cretaceous molluscan biostratigraphy and biogeography, Western Interior Basin, North America, in *Evolution of the Western Interior Basin*, edited by C. G. E. Caldwell and E. G. Kauffman, *Geol. Assoc. Can. Spec. Paper*, 39, 397–434.
- Kerr, A. C., J. Tarney, P. D. Kempton, M. Pringle, and A. Nivia (2004), Mafic pegmatites intruding oceanic plateau gabbros and ultramafic cumulates from Bolivar, Colombia: Evidence for a “wet” mantle plume?, *J. Petrol.*, 45, 1877–1906.
- Kuhnt, W., and J. Wiedmann (1995), Cenomanian-Turonian source rock: Palaeobiogeographic and paleoenvironmental aspects, in *Palaeogeography, Palaeoclimatology and Source Rocks*, edited by A. Y. Huc, *AAPG Stud. Geol.*, 40, 213–231.
- Larson, R. L. (1991a), Latest pulse of Earth: Evidence for a mid-Cretaceous superplume, *Geology*, 19, 547–550.
- Larson, R. L. (1991b), Geological consequences of superplumes, *Geology*, 19, 963–966.
- Larson, R. L., and E. Erba (1999), Onset of the mid-Cretaceous greenhouse in the Barremian-Aptian: Igneous events and the biological, sedimentary, and geochemical responses, *Paleoceanography*, 14, 663–678.
- Leckie, R. M. (1985), Foraminifera of the Cenomanian-Turonian boundary interval, Greenhorn Formation, Rock Canyon Anticline, Pueblo, Colorado, in *Fine-Grained Deposits and Biofacies of the Cretaceous Western Interior Seaway: Evidence of Cyclic Sedimentary Processes*, *Field Trip Guideb.* 4, edited by L. M. Pratt et al., pp. 139–149, Soc. of Sediment. Geol., Tulsa, Okla.
- Leckie, R. M. (1989), An oceanographic model for the early evolutionary history of planktonic foraminifera, *Palaeogeogr. Palaeoclimatol. Palaeoecol.*, 73, 107–138.
- Leckie, R. M., R. F. Yuretic, O. L. O. West, D. Finkelstein, and M. Schmidt (1998), Paleoceanography of the southwestern Western Interior Sea during the time of the Cenomanian-Turonian boundary (Late Cretaceous), in *Stratigraphy and Paleoenvironments of the Cretaceous Western Interior Seaway, USA, Concepts Sedimentol. Paleontol.*, vol. 6, edited by W. E. Dean and M. A. Arthur, pp. 101–126, Soc. of Sediment. Geol., Tulsa, Okla.
- Leckie, R. M., T. J. Bralower, and R. Cashman (2002), Oceanic anoxic events and plankton evolution: Biotic response to tectonic forcing during the mid-Cretaceous, *Paleoceanography*, 17(3), 1041, doi:10.1029/2001PA000623.
- Lupton, J. E., E. T. Baker, and G. J. Massoth (1999), Helium, heat and generation of hydrothermal event plumes at mid-ocean ridges, *Earth Planet. Sci. Lett.*, 171, 343–350.
- McArthur, J. M., W. J. Kennedy, M. Chen, M. F. Thirlwall, and A. S. Gale (1994), Strontium isotopic stratigraphy for the Late Cretaceous time: Direct numerical calibration of the Sr isotope curve based on the US western interior, *Palaeogeogr. Palaeoclimatol. Palaeoecol.*, 108, 95–119.
- Meyers, S. R., B. B. Sageman, and L. A. Hinnov (2001), Integrated quantitative stratigraphy of the Cenomanian-Turonian Bridge Creek limestone member using evolutive harmonic analysis and stratigraphic modeling, *J. Sediment. Res.*, 71, 628–644.
- Milnes, A. R., and R. W. Fitzpatrick (1989), Titanium and zirconium minerals, in *Minerals in Soil Environments*, vol. 23, edited by J. B. Dixon and S. B. Weed, pp. 1131–1205, Soil Sci. Soc. Am., Madison, Wisc.
- Morgan, W. J. (1981), Hotspot tracks and the opening of the Atlantic and Indian oceans, in *The Oceanic Lithosphere, The Sea*, edited by C. Emiliani, pp. 443–487, John Wiley, Hoboken, N. J.
- Obradovich, J. D. (1993), A Cretaceous time-scale, in *Evolution of the Western Interior Basin*, edited by W. G. E. Caldwell and E. G. Kauffman, *Geol. Assoc. Can. Spec. Pap.*, 39, 379–396.
- Orth, C. J., M. J. Attrep, L. R. Quintana, W. P. Elder, E. G. Kauffman, R. Diner, and T. Villamil (1993), Elemental abundance anomalies in the late Cenomanian extinction interval: A search for the source(s), *Earth Planet. Sci. Lett.*, 117, 189–204.
- Pratt, L. M. (1984), Influence of paleoenvironmental factors on the preservation of organic matter in Middle Cretaceous Greenhorn Formation near Pueblo, Colorado, *AAPG Bull.*, 68, 1146–1159.
- Pratt, L. M. (1985), Isotopic studies of organic matter and carbonate in rocks of the Greenhorn marine cycle, in *Fine-Grained Deposits and Biofacies of the Cretaceous Western Interior Seaway: Evidence of Cyclic Sedimentary Processes*, edited by L. M. Pratt, E. G. Kauffman, and F. B. Zelt, *Field Trip Guideb.* 4, pp. 38–48, Soc. of Sediment. Geol., Tulsa, Okla.
- Pratt, L. M., and C. N. Threlkeld (1984), Stratigraphic significance of $^{13}\text{C}/^{12}\text{C}$ ratios in mid-Cretaceous rocks of the western interior, U.S.A., in *The Mesozoic of Middle North America*, edited by D. F. Stott and D. J. Glass, *Mem. Can. Soc. of Pet. Geol.*, 9, 305–312.
- Pratt, L. M., D. A. Arthur, W. E. Dean, and P. A. Scholle (1993), Paleoceanographic cycles and events during the Late Cretaceous in the Western Interior Seaway of North America, in *Evolution of the Western Interior Basin*, edited by W. G. E. Caldwell and E. G. Kauffman, *Geol. Assoc. Can. Spec. Pap.*, 39, 333–354.
- Premoli Silva, I., and W. V. Sliter (1999), Cretaceous paleoceanography: Evidence from planktonic foraminiferal evolution, in *The Evolution of Cretaceous Ocean-Climate System*, edited by E. Barrera and C. C. Johnson, *Spec. Pap. Geol. Soc. Am.*, 332, 301–328.
- Premoli Silva, I., E. Erba, G. Salvini, D. Verga, and C. Locatelli (1999), Biotic changes in Cretaceous anoxic events, *J. Foraminiferal Res.*, 29, 352–370.
- Richards, M. A., R. A. Duncan, and V. E. Courtillot (1989), Flood basalts and hotspot tracks: Plume heads and tails, *Science*, 246, 103–107.
- Rubin, K. (1997), Degassing of metals and metalloids from erupting seamount and mid-ocean ridge volcanoes: Observations and predictions, *Geochim. Cosmochim. Acta*, 61, 3525–3542.
- Sageman, B. B., and M. A. Arthur (1994), Early Turonian paleogeographic/paleobathymetric map, western interior, U.S., in *Mesozoic Systems of the Rocky Mountain Ranges, USA*, edited by M. V. Caputo et al., pp. 457–470, Soc. of Econ. Paleontol. Mineral., Tulsa, Okla.
- Sageman, B. B., J. Rich, M. A. Arthur, W. E. Dean, C. E. Savrda, and T. J. Bralower (1998), Multiple Milankovitch cycles in the Bridge Creek Limestone (Cenomanian-Turonian), Western Interior Basin, in *Stratigraphy and Paleoenvironments of the Cretaceous Western Interior Seaway, USA, Concepts Sedimentol. Paleontol.*, vol. 6, edited by W. E. Dean and M. A. Arthur, pp. 153–171, Soc. of Sediment. Geol., Tulsa, Okla.
- Saltzman, E. S., and E. J. Barron (1982), Deep circulation in the Late Cretaceous: Oxygen isotope paleotemperature from *Inoceramus* remains in D.S.D.P. cores, *Palaeogeogr. Palaeoclimatol. Palaeoecol.*, 40, 167–181.
- Schlanger, S. O., and H. C. Jenkyns (1976), Cretaceous oceanic anoxic events: Causes and consequences, *Geol. Mijnbouw*, 55, 179–184.
- Schlanger, S. O., M. A. Arthur, H. C. Jenkyns, and P. A. Scholle (1987), The Cenomanian-Turonian ocean anoxic event: Stratigraphy

- and distribution of carbon-rich beds and the marine $\delta^{13}\text{C}$ excursion, *Geol. Soc. Spec. Publ. London*, 26, 371–399.
- Scholle, P. A., and M. A. Arthur (1980), Carbon isotope fluctuation in Cretaceous pelagic limestones: Potential stratigraphic and petroleum exploration tool, *AAPG Bull.*, 64, 67–87.
- Sen, G., R. Hickey-Vargas, D. G. Waggoner, and F. Maurasse (1988), Geochemistry of basalts from the Dumisseau Formation, southern Haiti: Implications for the origin of the Caribbean Sea crust, *Earth Planet. Sci. Lett.*, 87, 423–437.
- Sinton, C. W., and R. A. Duncan (1997), Potential links between ocean plateau volcanism and global ocean anoxia at the Cenomanian-Turonian boundary, *Econ. Geol.*, 92, 836–842.
- Sinton, C. W., R. A. Duncan, M. Storey, J. Lewis, and J. J. Estrada (1998), An oceanic flood basalt province within the Caribbean plate, *Earth Planet. Sci. Lett.*, 155, 221–235.
- Sunda, W. G., and S. A. Huntsman (1996), Antagonisms between cadmium and zinc toxicity and manganese limitation in a coastal diatom, *Limnol. Oceanogr.*, 41, 373–387.
- Swanson, D. A., T. L. Wright, and R. T. Helz (1975), Linear vent systems and estimated rates of magma production and eruption for the Yakima basalt on the Columbia Plateau, *Am. J. Sci.*, 275, 877–905.
- Tejada, M. L. G., J. J. Mahoney, R. A. Duncan, and M. P. Hawkins (1996), Age and geochemistry of basement and alkalic rocks of Malaita and Santa Isabel, Solomon Island, southern margin of Ontong Java plateau, *J. Petrol.*, 37, 361–394.
- Tsikos, H., H. C. Jenkyns, B. Walsworth-Bell, M. R. Petrizzo, A. Forster, S. Kolonic, E. Erba, I. Premoli Silva, M. Baas, T. Wagner, and J. S. Sinninghe Damste (2004), Carbon-isotope stratigraphy recorded by the Cenomanian-Turonian oceanic anoxic event: Correlation and implications based on three key localities, *J. Geol. Soc. London*, 161, 711–719.
- Vogt, P. R. (1989), Volcanogenic upwelling of anoxic, nutrient-rich water: A possible factor in Carbonate-bank/reef demise and benthic faunal extinctions, *Geol. Soc. Am. Bull.*, 101, 1225–1245.
- Wignall, P. B. (1994), *Black Shales*, 127 pp., Oxford Univ. Press, New York.

T. J. Bralower, Department of Geosciences, Pennsylvania State University, University Park, PA 16802, USA. (bralower@geosc.psu.edu)

R. A. Duncan, College of Oceanic and Atmospheric Sciences, Oregon State University, Corvallis, OR 97331-5503, USA. (rduncan@coas.oregonstate.edu)

L. J. Snow, National Science Foundation, 4201 Wilson Blvd., Arlington, VA 22230, USA. (lsnow@nsf.gov)